EVALUATION OF MASSLESS-SPRING MODELING OF SUSPENSION-LINE ELASTICITY DURING THE PARACHUTE UNFURLING PROCESS

by Lamont R. Poole and Earle K. Huckins III

Langley Research Center
Hampton, Va. 23365

NATIONAL AERONAUTICS AND SPACE ADMINISTRATION • WASHINGTON, D. C. • FEBRUARY 1972

1. Report No. NASA TN D-6671	2. Government Accession No.	3. Recipient's Catalog No.
4. Title and Subtitle EVALUATION OF MASSLESS-SPRING MODELING OF SUSPENSION-LINE ELASTICITY DURING THE PARACHUTE UNFURLING PROCESS		5. Report Date February 1972 6. Performing Organization Code
7. Author(s) Lamont R. Poole and Earle K. Huckins III		8. Performing Organization Report No. L-8097
9. Performing Organization Name and Address NASA Langley Research Center Hampton, Va. 23365		10. Work Unit No. 815-20-09-03 11. Contract or Grant No.
12. Sponsoring Agency Name and Address National Aeronautics and Space Administration Washington, D.C. 20546		13. Type of Report and Period Covered Technical Note 14. Sponsoring Agency Code
15. Supplementary Notes		

16. Abstract

A general theory on mathematical modeling of elastic parachute suspension lines during the unfurling process was developed. Massless-spring modeling of suspension-line elasticity was evaluated in detail. For this simple model, equations which govern the motion were developed and numerically integrated. The results were compared with flight test data. In most regions, agreement was satisfactory. However, poor agreement was obtained during periods of rapid fluctuations in line tension.

17. Key Words (Suggested by Author(s)) Parachute deployment Suspension-line elasticity	18. Distribution Statement Unclassified – Unlimited

19. Security Classif. (of this report) Unclassified	20. Security Classif. (of this page) Unclassified	21. No. of Pages 30	22. Price* $3.00

*For sale by the National Technical Information Service, Springfield, Virginia 22151

EVALUATION OF MASSLESS-SPRING MODELING OF SUSPENSION-LINE ELASTICITY DURING THE PARACHUTE UNFURLING PROCESS

By Lamont R. Poole and Earle K. Huckins III
Langley Research Center

SUMMARY

Mathematical modeling of elasticity in parachute suspension lines during the unfurling process was investigated. The massless-spring approximation was evaluated in depth. Equations which govern the elastic response of the suspension lines for this basic model were combined with equations governing the motion of the vehicle and the deployment bag. This set of governing equations was integrated numerically and the results were compared with flight test data. Agreement was satisfactory except during periods of rapid fluctuations in line tension. Lack of agreement during these periods was attributed primarily to omission of wave mechanics in the suspension-line elasticity model under evaluation.

INTRODUCTION

Parachute deployment is defined as the process of extending the parachute canopy and suspension lines to a point at which satisfactory inflation can occur. Interest in decelerator systems for planetary entry vehicles has stimulated research in deployment dynamics which has resulted in significant improvements over earlier empirical methods (refs. 1 and 2). A primary need for simulating the lines-first deployment process is to determine the motion of the deployment bag relative to the towing vehicle. Knowledge of sequence of events and deployment times is important from a mission-analysis standpoint. A greater understanding of the process by which the packed parachute is unfurled is important in deployment system design. An accurate prediction of the tension developed in the suspension lines during lines-first deployment is important from a standpoint of vehicle motions.

An analysis of the lines-first deployment process for an inelastic parachute was presented in reference 3. The analysis presented in reference 4 indicated that the effects of suspension-line elasticity can be significant during deployment. The effects of suspension-line elasticity during the parachute inflation process have been studied previously (ref. 5) for a simple two-body spring-mass system. Mathematical modeling of

elastic suspension lines during the unfurling process is discussed in appendix A. The purpose of the present paper is to evaluate the use of a simple massless-spring model in the analysis of lines-first deployment dynamics.

In the present paper, equations are developed which, for a lines-first forced-ejection deployment, govern the planar motion of the vehicle, the linear motion of the deployment bag relative to the vehicle, and the unfurling process. In the development, the parachute suspension lines are represented by a variable-length massless spring. The usefulness of this mathematical model is evaluated by employing it in the calculation of deployment motions and loads of two disk-gap-band parachute deployment flight tests. Uncertainty in the mechanisms by which the packed parachute is unfurled from the deployment bag is accounted for by using both precise and averaged linear-mass-density distributions for each of the parachutes.

SYMBOLS

A	reference area, meters
c	wave propagation velocity of suspension lines, meters/second
C	damping coefficient of a single suspension line, newton-seconds
C_D	drag coefficient, $\frac{\text{Drag}}{q_\infty A}$
F_D'	aerodynamic drag per unit length of suspension lines, newtons/meter
F_{re}	unfurling resistance force, newtons
g	acceleration due to gravity, meters/second^2
h	altitude, meters
K'_{sec}	specific secant modulus of a single suspension line, newtons
l	general spatial coordinate along unstressed suspension lines, measured from vehicle attachment point, meters
l_B	unfurled length (or, equivalently, spatial coordinate of parachute mass element exiting mouth of deployment bag), meters

L_p	total unstressed length of extended parachute, meters
L_{sl}	total unstressed length of suspension lines, meters
m	mass, kilograms
m'	linear mass density of general element (parachute) exiting mouth of deployment bag, kilograms/meter
m'_{sl}	linear mass density of a single suspension line, kilograms/meter
n_{sl}	number of suspension lines
q_∞	free-stream dynamic pressure, newtons/meter^2
t	time, seconds
T	tension, newtons
u	unfurling velocity or rate at which parachute exits mouth of deployment bag, meters/second
v	velocity, meters/second
ΔV	ejection velocity, meters/second
x	deployed distance relative to vehicle, meters
γ	vehicle flight-path angle, degrees
δ	displacement of any cross section of suspension lines from its unstressed position, meters
ϵ	strain, meters/meter
η	wake parameter (ratio of drag coefficient of deployment bag in vehicle wake to that in free stream)

ρ_∞ free-stream density, kilograms/meter^3

ω effective loading frequency, radians/second

Subscripts:

b deployment bag

B deployment-bag mouth

dyn dynamic

e deployment bag plus its instantaneous contents

o conditions at beginning of deployment

s static

v vehicle

V suspension-line attachment point at vehicle

Dots over symbols denote time derivatives.

ANALYSIS

In the analysis to follow, equations which govern the dynamics of lines-first deployment of a parachute having elastic suspension lines of the massless-spring class are developed. Equations which govern the motion of the vehicle and the deployment bag are presented. An expression for the rate at which the parachute exits the mouth of the deployment bag (the unfurling rate) is given. In addition, equations are presented by which the elastic behavior of the suspension lines can be approximated.

A typical vehicle-parachute configuration during a deployment of the lines-first type (ref. 4) is shown in figure 1. A sketch of the forces affecting the dynamics of the deployment process is given in figure 2. For the purposes of the present analysis, the surface of the earth is assumed flat, and surface-relative accelerations are considered inertial.

Motion of the Vehicle

The motion of the vehicle is influenced by aerodynamic forces, tension in the parachute suspension lines, and gravitational attraction. Assume that

(1) The vehicle can be represented by a mass particle (vehicle moments of inertia are neglected).

(2) The suspension-line tension at the vehicle is parallel to the vehicle relative wind.

(3) The vehicle is nonlifting.

(4) Winds are negligible.

Under these assumptions, the longitudinal acceleration of the vehicle is given by

$$\dot{v}_V = -\left[\frac{\left(C_D A\right)_V q_\infty + T_V}{m_V} + g \sin \gamma\right] \tag{1}$$

where

$\dot{v}$ inertial acceleration

C_D drag coefficient

A reference area

q_∞ free-stream dynamic pressure $\left(q_\infty = \frac{1}{2}\rho_\infty v_V^2\right)$

ρ_∞ free-stream density

T_V tension at suspension-line attachment point on vehicle

m mass

g acceleration due to gravity

γ vehicle flight-path angle

and subscript

v vehicle

In order to completely specify the earth-relative planar motion of the vehicle, the following additional trajectory equations are required:

$$\dot{h}_V = v_V \sin \gamma \tag{2}$$

$$\dot{\gamma} = - \frac{g \cos \gamma}{v_V} \tag{3}$$

where $\dot{h}_V$ is the time rate of change of the altitude of the vehicle.

Motion of the Deployment Bag

The motion of the deployment bag can be closely approximated by introducing the following additional assumptions:

(1) The deployment bag and its instantaneous contents can be represented by a variable-mass particle. (Moments of inertia are neglected.)

(2) The velocity vector of the deployment bag relative to the vehicle is parallel to the relative-wind velocity vector of the vehicle.

(3) The reduction in dynamic pressure acting on the deployment bag due to the motion of the bag relative to the vehicle is neglected.

Under these assumptions, the longitudinal acceleration of the deployment bag relative to the inertial frame is given by

$$\dot{v}_b = - \left[\frac{\eta (C_D A)_b q_\infty - F_{re}}{m_e} + g \sin \gamma \right] \tag{4}$$

where

η wake parameter

F_{re} unfurling resistance force

and subscripts

b deployment bag

e deployment bag plus its instantaneous contents

In addition, the velocity of the deployment bag relative to the vehicle can be written as follows:

$$\dot{x}_b = v_v - v_b \tag{5}$$

Unfurling Rate

A relationship between the tension in the unfurling parachute at the mouth of the deployment bag and the unfurling rate was given in reference 4, and can be written as

$$T_B = m'u^2 + F_{re} \tag{6}$$

where

T_B tension in unfurling parachute at mouth of deployment bag

m' linear mass density of parachute exiting mouth of deployment bag

u rate at which parachute exits mouth of deployment bag (unfurling rate)

and

$$u = \dot{l}_B \tag{7}$$

or, by using equation (6),

$$\dot{l}_B = \left(\frac{T_B - F_{re}}{m'}\right)^{1/2} \tag{8}$$

Suspension-Line Elasticity

In order to completely define the motion of the deployment process, it is necessary to formulate a relationship between the suspension-line tension at the vehicle, the tension at the mouth of the deployment bag, the motion of the deployment bag relative to the vehicle, the unfurling rate, and the unstressed length of the unfurled parachute. This relationship is furnished by a mathematical model of the suspension-line elasticity.

Mathematical modeling of elastic suspension lines is discussed in appendix A. It is shown that, under the following assumptions, the elastic suspension lines can be approximated by a massless spring of variable length:

(1) Throughout the deployment process, the suspension lines are under tension.

(2) Aerodynamic drag on the unfurled suspension lines is negligible.

(3) Suspension-line tension is independent of strain rate. (Viscous damping is neglected.)

(4) Linear mass density of the suspension lines is negligible.

(5) The effective loading frequency is much less than the effective propagation frequency. (See appendix A.)

The tension throughout the suspension lines is constant at any particular time:

$$T = T_V = T_B \tag{9}$$

where T is the tension at any arbitrary spatial location along the unfurled suspension lines and is given by

$$T = n_{sl} K'_{sec} \epsilon \tag{10}$$

where

n_{sl} number of suspension lines

K'_{sec} specific secant modulus of a single suspension line

ϵ strain in suspension lines

The suspension-line strain is by definition

$$\epsilon = \frac{x_B - l_B}{l_B} \qquad \left(0 < l_B < L_{sl}\right) \tag{11}$$

$$\epsilon = \frac{x_B - l_B}{L_{sl}} \qquad \left(L_{sl} < l_B < L_p\right) \tag{12}$$

where

x_B deployed distance (distance from suspension-line attachment point on vehicle to deployment-bag mouth) $\left(\text{Note: } \dot{x}_B = \dot{x}_b\right)$

L_{sl} total unstressed length of suspension lines

L_p total unstressed length of extended parachute

RESULTS AND DISCUSSION

A mathematical model to describe precisely the dynamics of the entire parachute deployment sequence would necessarily involve direct solution of the partial differential equations governing the wave motion of the suspension lines. In the present paper, the consequences of neglecting wave mechanics were studied by evaluating a massless-spring model of suspension-line elasticity.

In order to evaluate the accuracy obtained by using this simple model, it was used to calculate the deployment motions for two flight tests of disk-gap-band parachutes: the second balloon-launched flight test of the NASA Planetary Entry Parachute Program (ref. 6) and the first flight test of the NASA Supersonic Planetary Entry Decelerator Program (ref. 7). The governing equations, in conjunction with the auxiliary expressions described in appendix B, were solved numerically on a digital computer, using a fifth-order Runge-Kutta integration technique, for appropriate values of parameters and coefficients. In order to allow for uncertainties in the mechanisms by which the packed parachute is unfurled from the deployment bag, two linear mass distributions for each parachute were employed in the solution: a precise mass distribution (of the form shown in sketch B1 of appendix B) and a distribution consisting of averaged values of linear mass density (average of the precise values over a characteristic parachute folding length, the deployment-bag diameter).

Calculated histories of unfurled length for the two flight tests are presented in figure 3 and compared with test data points, for which occurrence times have been adjusted to account for wave propagation times. As neither of the calculated histories was affected significantly by the alternate mass distribution, only one such history is presented for each flight. The flight test data points presented correspond to mortar fire, line stretch, and estimated bag strip (ref. 8). The calculated histories show good agreement with flight test data.

Calculated histories of tension for the two flight tests are presented and compared with test data in figure 4. Again, neither of the calculated histories was significantly affected by the alternate mass distribution, and only one tension history is presented for each flight. The initial large peak in each flight test data history corresponds to the impact of a tensiometer, which was included in the flight system in order to measure tension levels. This occurrence was not considered in the present mathematical model. Agreement is acceptable except during the periods corresponding to the unfurling of the band portions of the respective canopies. Lack of agreement during these periods of rapid load fluctuations is attributed to omission of wave mechanics in the suspension-line elasticity model.

Calculated histories of the deployment rate and unfurling rate using both precise and averaged linear mass distributions are presented in figure 5 for the flight test of reference 6 and in figure 6 for the flight test of reference 7. Similar trends are exhibited in each figure. The deployment-bag motion is quite smooth in nature, independent of the choice of linear mass distribution. In general, the unfurling rate history closely follows the deployment rate history. However, sharp decreases in the unfurling rate occur when sudden increases in the linear mass density of the unfurling parachute are encountered; conversely, sharp increases in unfurling rate occur when sudden decreases in linear mass density are encountered. The effect of averaging the linear mass density over a characteristic length is virtually to eliminate the narrow "spikes" in the precise mass distribution which are representative of cloth overlapping and tape reinforcement in the parachute canopy. As a consequence, the magnitudes of the decreases in unfurling rate are reduced when the averaged mass distribution is used. The increases in unfurling rate, which occur as the gap and vent portions of the canopy unfurl from the bag, are not affected significantly by the alternate mass distribution. As the gap emerges from the bag, the unfurling rate actually exceeds the ejection velocity of the respective flight tests. In consideration of the relatively poor agreement of calculated tension histories with flight test data and the absence of data concerning unfurling rate, some uncertainty exists as to the magnitudes of the calculated maxima and minima in unfurling rate. However, the trends exhibited in the calculated histories are representative of the physical situation.

CONCLUSIONS

Massless-spring modeling of suspension-line elasticity during the lines-first parachute unfurling process has been studied. Based on numerical solution of the governing equations for two disk-gap-band parachute deployment flight tests, the following conclusions can be made in evaluation of the present model:

1. Calculated histories of unfurled length were not affected significantly by either the elastic model or the alternate parachute linear mass distributions and agreed very well with flight test data.

2. Calculated tension histories agreed poorly with flight test data during periods corresponding to the unfurling of the band portion of the canopies. Acceptable agreement was obtained during periods corresponding to suspension-line and disk unfurling. Tension histories were not affected significantly by the alternate linear mass distributions.

3. Calculated histories of unfurling rate exhibited fluctuation about the smooth deployment rate histories, generally as a function of the selected linear mass distribution. Inasmuch as the local maxima in the unfurling rate histories were not affected

significantly by the alternate mass distributions, there exists the possibility that unfurling rates of greater magnitude than the flight-test ejection velocities were experienced during the periods corresponding to unfurling of the gap portion of the respective canopies.

4. In light of the high-frequency loading experienced during canopy unfurling, a formulation which considers the wave mechanics of the suspension lines will probably be required in order to reduce the remaining inaccuracies and to clear up existing uncertainties in the unfurling process.

Langley Research Center,
National Aeronautics and Space Administration,
Hampton, Va., January 3, 1972.

APPENDIX A

MATHEMATICAL MODELING OF PARACHUTE SUSPENSION LINES

Mathematical models of parachute suspension lines can vary greatly in complexity. The motion of the suspension lines during deployment can be determined in detail by writing Newton's second law for an element of the lines, formulating an elastic model for the element, and integrating the resulting set of coupled nonlinear partial differential equations. The results obtained would completely describe the lateral and longitudinal motions of the suspension lines.

However, this degree of complexity is not usually required since, in many cases, the deployment motion is approximately one-dimensional. Under the assumption of linear motion, the governing equations reduce to a single nonlinear partial differential equation which describes the longitudinal wave motion in the suspension lines. This substantial reduction in the complexity of the analysis introduces relatively small inaccuracies in the results. Linear motion will be assumed in the analysis to follow.

The elastic state of the suspension lines can be represented by use of the coordinates and variables shown in sketch A1.

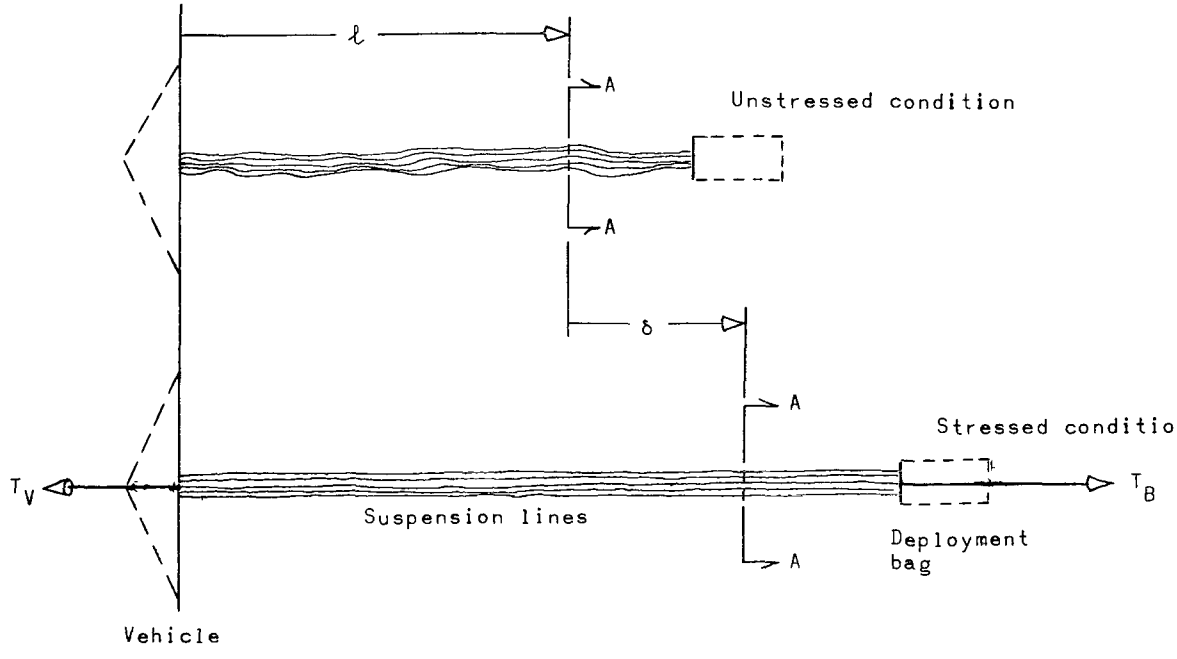

Sketch A1

The longitudinal forces acting on an element of the suspension lines are shown as follows:

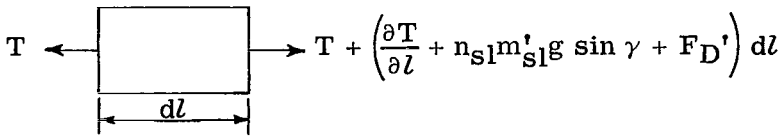

where

T tension in element

m'_{sl} linear mass density of a single suspension line

n_{sl} number of suspension lines

g acceleration due to gravity

γ vehicle flight-path angle

F_D' aerodynamic drag per unit length of suspension lines

Assuming linear motion, Newton's second law for the longitudinal motion of the line element can be written as

$$\frac{\partial T}{\partial l} + n_{sl} m'_{sl} g \sin\gamma + F_D' = n_{sl} m'_{sl} \left(\frac{\partial^2 \delta}{\partial t^2} - \dot{v}_V\right) \tag{A1}$$

where $\dot{v}_V$ is the inertial acceleration of the vehicle given by

$$\dot{v}_V = -\left[\frac{(C_D A)_V q_\infty + T_V}{m_V} + g \sin\gamma\right] \tag{A2}$$

where

C_D drag coefficient

A reference area

q_∞ free-stream dynamic pressure

and subscript

v vehicle

The governing equation for the motion of the element can be obtained by substituting equation (A2) in equation (A1). The result can be written

$$\frac{\partial^2 \delta}{\partial t^2} - \frac{1}{n_{sl} m'_{sl}} \frac{\partial T}{\partial \ell} = \frac{F_D'}{n_{sl} m'_{sl}} - \frac{\left(C_D A\right)_v q_\infty + T_V}{m_v} \tag{A3}$$

In order to define the motion completely, it is necessary to determine a functional relationship between the tension, the displacement δ, and its derivatives. The tension in the line element is a result of static tension T_s and tension due to dynamic effects T_{dyn}; that is,

$$T = T_s + T_{dyn} \tag{A4}$$

The static tension can be related to the strain in the following manner:

$$T_s = n_{sl} K'_{sec} \epsilon \tag{A5}$$

where

ϵ strain $\left(\epsilon = \frac{\partial \delta}{\partial \ell}\right)$

K'_{sec} specific secant modulus of a single suspension line

n_{sl} number of suspension lines

Note that, in general, the secant modulus is a function of the strain and the strain history; and, as such, it can include the effects of nonlinear elasticity, mechanical hysteresis, and permanent set.

In a similar manner, the tension due to dynamic effects can be related to the strain rate as follows:

$$T_{dyn} = n_{sl} C \dot{\epsilon} \tag{A6}$$

where C is the damping coefficient of a single suspension line. In general, the damping coefficient is a function of both the strain and the strain rate. This nonlinear function of strain rate accounts for elastic hysteresis (the elastic aftereffect) and viscous (or rate) damping.

The tension gradient in equation (A3) can now be written in terms of the displacement gradients and their time derivatives by use of equations (A5) and (A6). The result is

$$\frac{\partial T}{\partial l} = n_{sl}\left[K'_{sec}\frac{\partial^2\delta}{\partial l^2} + \frac{\partial K'_{sec}}{\partial l}\frac{\partial\delta}{\partial l} + C\frac{\partial}{\partial t}\left(\frac{\partial^2\delta}{\partial l^2}\right) + \frac{\partial C}{\partial l}\frac{\partial}{\partial t}\left(\frac{\partial\delta}{\partial l}\right)\right] \tag{A7}$$

Initial conditions on the motion are as follows:

(1) The initial displacement profile of the suspension lines.

(2) The initial displacement rate profile of the suspension lines.

In addition, the dynamic response is subject to the following boundary conditions:

(1) The displacement at the vehicle

$$\delta\Big|_{l=0} = 0 \tag{A8}$$

(2) The displacement rate at the mouth of the deployment bag

$$\frac{\partial\delta}{\partial t}\Big|_{l=l_B} = \dot{x}_b - u \tag{A9}$$

where

l_B spatial coordinate of mass element exiting deployment-bag mouth

u unfurling velocity

$\dot{x}_b$ velocity of bag relative to vehicle

(3) The tension at the mouth of the deployment bag

$$T_B = m'u^2 + F_{re} \tag{A10}$$

where

T_B tension in element unfurling from deployment bag

m' linear mass density of unfurling element

F_{re} unfurling resistance

A simultaneous solution to equations (A3) and (A7) subject to the initial and boundary conditions listed above will completely define the elastic state of the suspension lines.

In most cases, a solution of the complete system of equations can only be obtained numerically. A suggested procedure is to approximate partial derivatives by difference quotients formed from the finite difference in elastic states of adjacent elements. Finite difference schemes for solution of partial differential equations are discussed in many textbooks on numerical analysis. (For example, see ref. 9.)

The governing equations can be simplified considerably by neglecting damping and assuming that the elastic and mass properties are the same at all cross sections along the suspension lines. Under these assumptions, equations (A3) and (A7) can be combined and reduced to

$$\frac{\partial^2\delta}{\partial t^2} - \frac{K'_{sec}}{m'_{sl}}\frac{\partial^2\delta}{\partial \ell^2} = \frac{F_D'}{n_{sl}m'_{sl}} - \frac{\left(C_DA\right)_V q_\infty + T_V}{m_V} \tag{A11}$$

For linearly elastic suspension lines $\left(K'_{sec} = \text{Constant}\right)$, the wave velocity can be introduced:

$$c^2 = \frac{K'_{sec}}{m'_{sl}} \tag{A12}$$

where c is the longitudinal wave velocity.

For linearly elastic suspension lines, negligible drag on the unfurling suspension line, infinite vehicle mass, and constant m'_{sl}, equation (A11) reduces to the one-dimensional wave equation which has a classical solution. In reference 4, the classical solution, for a particular set of initial and boundary conditions, was used to predict the "snatch force" which occurs as the canopy skirt emerges from the deployment bag.

Variations in the linear mass density of the material exiting the mouth of the deployment bag result in load fluctuations in the suspension lines. During events such as line stretch, the effective frequency of these load fluctuations can be relatively high. As a

result, a loading cycle may be completed before the response wave has traversed the entire length of the suspension lines. In order to accurately model the suspension lines during such an event, wave mechanics must be considered. However, during periods in which the effective loading frequency is much less than the effective propagation frequency, that is,

$$\omega << \frac{c}{L_{sl}} \tag{A13}$$

where

ω effective loading frequency

c wave velocity $\left(c^2 = \frac{K'_{sec}}{m'_{sl}}\right)$

L_{sl} length of unfurled suspension lines

the wave velocity may be considered infinite. Infinite wave velocity implies either inextensible suspension lines $\left(K'_{sec} \to \infty\right)$ or massless suspension lines $\left(m'_{sl} \to 0\right)$.

For inextensible suspension lines, the displacement of the lines from the unstressed position is identically zero and equation (A3) reduces to

$$\frac{\partial T}{\partial l} = n_{sl} m'_{sl} \left[\frac{\left(C_D A\right)_v q_\infty + T_V}{m_V}\right] - F_D' \tag{A14}$$

which can be integrated to give the tension profile in the inextensible lines:

$$T = T_B - n_{sl} m'_{sl} \left[\frac{\left(C_D A\right)_v q_\infty + T_V}{m_V}\right]\left(l_B - l\right) - \int_{l_B}^{l} F_D' \, dl \tag{A15}$$

The inextensible model, simplified further by neglecting aerodynamic drag on the lines, was used to study the dynamics of the unfurling process in reference 3.

For massless suspension lines (note however, that the lines are assumed massless with respect to elastic modeling, not with respect to tension generation at the mouth of the deployment bag), equation (A11) reduces to

$$\frac{\partial^2 \delta}{\partial l^2} = - \frac{F_D'}{n_{sl} K'_{sec}} \tag{A16}$$

which can be written

$$\frac{\partial T}{\partial l} = -F_D' \tag{A17}$$

Assuming that the drag of the unfurled suspension lines is much less than the suspension-line tension, equation (A17) can be closely approximated by

$$\frac{\partial T}{\partial l} = 0 \tag{A18}$$

Therefore, under the assumption of vanishing linear mass density, tension is constant throughout the lines at any particular time.

The dynamic response of suspension lines during the unfurling process can be most accurately determined by using a mathematical model which includes wave mechanics. However, a numerical solution to the governing partial differential equation is considerably more complex than a numerical solution to the ordinary differential equations characteristic of the simpler models. Additional complexities may be introduced in a model which includes wave mechanics by the dispersion of the wave velocities between individual suspension lines. The purpose of the present analysis is to evaluate a massless-spring model of the suspension lines, since this represents the simplest model which includes the effects of elasticity.

APPENDIX B

AUXILIARY COMPUTATIONAL EXPRESSIONS

Based on the assumptions made, the governing equations which were developed in the analysis section of this report define the dynamics of the deployment process. However, in order to successfully adapt this system of equations to standard numerical integration techniques, several additional expressions must be developed. These include expressions for the unfurling acceleration and for initial values of the unfurling rate and unfurling acceleration. In addition, a technique must be developed to treat discontinuities in the linear mass density. Several procedures which have been found useful are described in this appendix.

Unfurling Acceleration

An expression for the unfurling rate was given in the analysis section and can be written

$$\dot{l}_B = u = \left(\frac{T - F_{re}}{m'}\right)^{1/2} \tag{B1}$$

where

$$T = n_{sl} K'_{sec} \epsilon \tag{B2}$$

and

$$\epsilon = \frac{x_B - l_B}{l_B} \qquad \left(0 < l_B < L_{sl}\right) \tag{B3}$$

or

$$\epsilon = \frac{x_B - l_B}{L_{sl}} \qquad \left(L_{sl} < l_B < L_p\right) \tag{B4}$$

An expression for the unfurling acceleration can be developed in terms of other known derivatives. This additional derivative was found to be necessary in order to minimize truncation error experienced with the use of a fifth-order Runge-Kutta numerical integration technique. By assuming that the unfurling rate is a function of strain, the elastic modulus, and the linear mass density, the unfurling acceleration can be found by substituting equation (B2) into equation (B1) and differentiating:

$$\dot{u} = \frac{\partial u}{\partial \epsilon}\dot{\epsilon}\left(1 + \frac{\partial u/\partial K'_{sec}}{\partial u/\partial \epsilon}\frac{dK'_{sec}}{d\epsilon} + \frac{\partial u/\partial m'}{\partial u/\partial \epsilon}\frac{dm'}{dl_B}\frac{dl_B}{d\epsilon}\right) \tag{B5}$$

Evaluating the partial derivatives, equation (B5) can be expressed as

$$\dot{u} = \frac{n_{sl}K'_{sec}}{2m'u}\dot{\epsilon}\left[1 + \frac{T}{n_{sl}\left(K'_{sec}\right)^2}\frac{dK'_{sec}}{d\epsilon} - \frac{1}{m'}\left(\frac{T + F_{re}}{n_{sl}K'_{sec}}\right)\left(\frac{l_B}{\frac{\dot{x}_B}{u} - \frac{x_B}{l_B}}\right)\frac{dm'}{dl_B}\right] \tag{B6}$$

For practical systems, the term,

$$\frac{T}{n_{sl}\left(K'_{sec}\right)^2}\frac{dK'_{sec}}{d\epsilon}$$

is of at least one order of magnitude less than 1. Therefore, equation (B6) can be reduced to

$$\dot{u} = \frac{n_{sl}K'_{sec}}{2m'u}\dot{\epsilon}\left[1 - \frac{1}{m'}\left(\frac{T + F_{re}}{n_{sl}K'_{sec}}\right)\left(\frac{l_B}{\frac{\dot{x}_B}{u} - \frac{x_B}{l_B}}\right)\frac{dm'}{dl_B}\right] \tag{B7}$$

where $\dot{u}$ is the unfurling acceleration, $\frac{dm'}{dl_B}$ is the slope of the linear-mass-density curve, and $\dot{\epsilon}$ is the strain rate, which is given by the derivatives of equations (B3) and (B4); that is,

$$\dot{\epsilon} = \frac{1}{l_B^2}\left(l_B\dot{x}_B - ux_B\right) \qquad \left(0 < l_B < L_{sl}\right) \tag{B8}$$

or

$$\dot{\epsilon} = \frac{\dot{x}_B - u}{L_{sl}} \qquad \left(L_{sl} < l_B < L_p\right) \tag{B9}$$

With the addition of equation (B7), the deployment motion is governed by seven first-order differential equations.

Initial Conditions

Initial values of the state variables of the vehicle and the deployment bag are well defined. However, since the initial values of the strain and the strain rate are undefined,

the initial values of the unfurling velocity and acceleration are also undefined. Expressions can be developed for these values by applying the limit theory expressed by L'Hospital's rule.

The strain during the initial unfurling sequence is defined as

$$\epsilon = \frac{x_B - l_B}{l_B} \tag{B10}$$

Therefore, the limiting value of strain at the initiation of deployment can be expressed

$$\epsilon_o = \frac{\Delta V}{u_o} - 1 \tag{B11}$$

where ΔV is the ejection velocity and the subscript o refers to the initial value. As shown previously, the suspension-line tension can be expressed in terms of the unfurling rate as

$$T = m'u^2 + F_{re} \tag{B12}$$

or in terms of the strain as

$$T = n_{sl} K'_{sec} \epsilon \tag{B13}$$

A cubic equation in the initial unfurling velocity can be found by equating equations (B12) and (B13), and evaluating the result at the initiation of deployment. The result can be written

$$u_o^3 + \frac{K'_{sec} + \frac{F_{re}}{n_{sl}}}{m'_{sl}} u_o - \frac{K'_{sec}}{m'_{sl}} \Delta V = 0 \tag{B14}$$

Equation (B14) can be solved for the initial unfurling velocity.

The strain rate during the initial unfurling sequence is given by

$$\dot{\epsilon} = \frac{1}{l_B^2}\left(l_B \dot{x}_B - u x_B\right) \tag{B15}$$

By successive application of L'Hospital's rule, the initial strain rate is determined to be

$$\dot{\epsilon}_o = \frac{u_o \ddot{x}_{B,o} - \dot{u}_o \dot{x}_{B,o}}{2u_o^2} \tag{B16}$$

where

$$\ddot{x}_{B,o} = \dot{v}_{v,o} - \dot{v}_{B,o} \tag{B17}$$

The initial unfurling acceleration can be determined by substituting equation (B16) into equation (B7). $\left(\text{Note that } \left.\frac{dm'}{dl_B}\right|_0 = 0.\right)$ The result can be expressed as

$$\dot{u}_o = \ddot{x}_{B,o} \frac{1}{\frac{\Delta V}{u_o} + \frac{4m'_{sl} u_o^2}{K'_{sec}}} \tag{B18}$$

where

$$\Delta V = \dot{x}_{B,o}$$

and

$$m'_{sl} = \frac{m'_o}{n_{sl}}$$

Discontinuities in Linear Mass Density

Sketch B1 shows a typical profile of a precise linear mass distribution for a disk-gap-band parachute. The "spikes" in the linear mass density are due to cloth overlapping

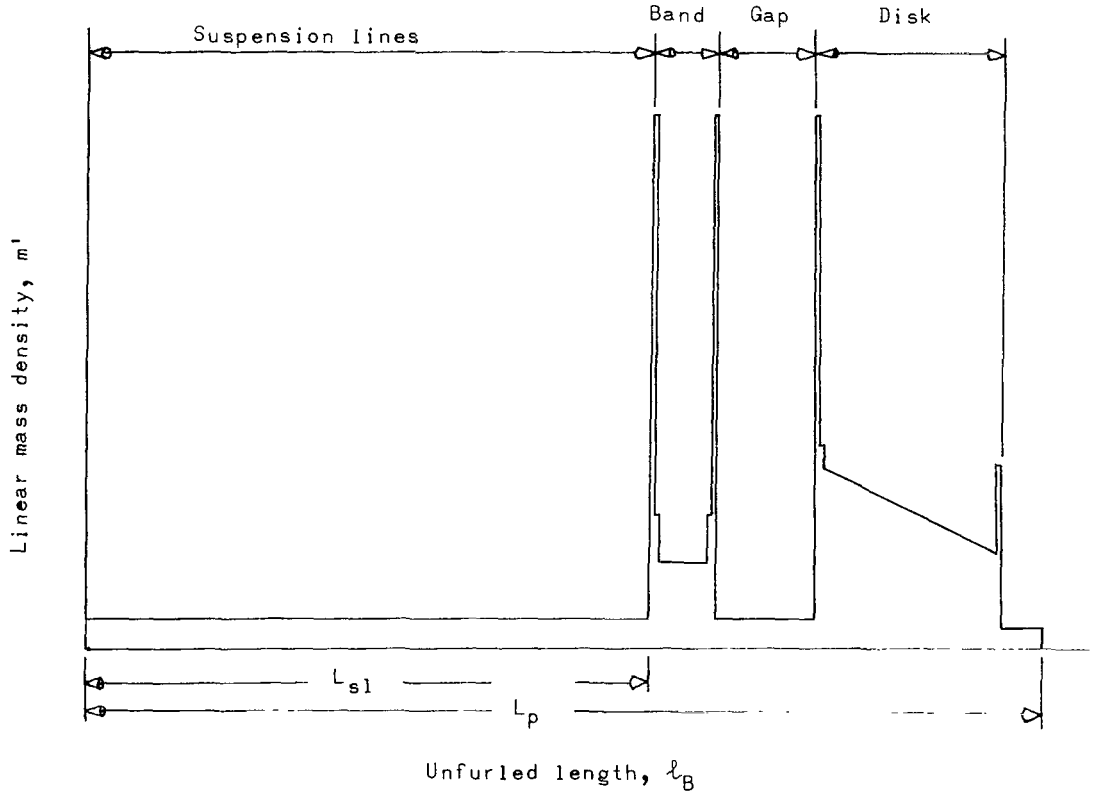

Sketch B1

and tape reinforcements in the canopy construction. These discontinuities in the linear mass density of the unfurling parachute result in a discontinuous unfurling rate. Recall the expression for the unfurling rate, which was expressed as

$$u = \left(\frac{T - F_{re}}{m'}\right)^{1/2} \tag{B19}$$

where

$$T = n_{sl} K'_{sec} \epsilon \tag{B20}$$

and

$$\epsilon = \frac{x_B - l_B}{l_B} \qquad \left(0 < l_B < L_{sl}\right) \tag{B21}$$

or

$$\epsilon = \frac{x_B - l_B}{L_{sl}} \qquad \left(L_{sl} < l_B < L_p\right) \tag{B22}$$

Since x_B and l_B are continuous functions of time, the tension must be a continuous function of time. The unfurling resistance has been experimentally shown to have an essentially constant value during the unfurling of the suspension lines and another essentially constant value during canopy unfurling. Therefore, discontinuities in the linear mass density, along with this single discontinuity in the unfurling resistance, introduce discontinuities in the unfurling rate. As a result, in order to integrate the unfurling acceleration correctly, the integral must be reinitialized at each discontinuity. This can be easily done owing to the continuous nature of the tension. The value of the unfurling rate following a discontinuity in the linear mass density is given by

$$u_2 = \left(\frac{T_1 - F_{re,2}}{m'_2}\right)^{1/2} \tag{B23}$$

where subscripts

1 denotes value of parameter prior to discontinuity

2 denotes value of parameter following discontinuity

REFERENCES

1. Broderick, M. A.; and Turner, R. D.: Design Criteria and Techniques for Deployment and Inflation of Aerodynamic Drag Devices. ASD Tech. Rep. 61-88, U.S. Air Force, Nov. 1961.

2. Amer. Power Jet Co.: Performance of and Design Criteria for Deployable Aerodynamic Decelerators. ASD-TR-61-579, U.S. Air Force, Dec. 1963. (Available from DDC as AD 429 921.)

3. Huckins, Earle K., III: Techniques for Selection and Analysis of Parachute Deployment Systems. NASA TN D-5619, 1970.

4. Huckins, Earle K., III: A New Technique for Predicting the Snatch Force Generated During Lines-First Deployment of an Aerodynamic Decelerator. AIAA Paper No. 70-1171, Sept. 1970.

5. Preisser, John S.; and Greene, George C.: Effect of Suspension Line Elasticity on Parachute Loads. J. Spacecraft Rockets, vol. 7, no. 10, Oct. 1970, pp. 1278-1280.

6. Bendura, Richard J.; Huckins, Earle K., III; and Coltrane, Lucille C.: Performance of a 19.7-Meter-Diameter Disk-Gap-Band Parachute in a Simulated Martian Environment. NASA TM X-1499, 1968.

7. Preisser, John S.; and Eckstrom, Clinton V.: Flight Test of a 40-Foot-Nominal-Diameter Disk-Gap-Band Parachute Deployed at a Mach Number of 1.91 and a Dynamic Pressure of 11.6 Pounds Per Square Foot. NASA TM X-1575, 1968.

8. Whitlock, Charles H.; and Bendura, Richard J.: Inflation and Performance of Three Parachute Configurations From Supersonic Flight Tests in a Low-Density Environment. NASA TN D-5296, 1969.

9. Crandall, Stephen H.: Engineering Analysis. McGraw-Hill Book Co., Inc., 1956.

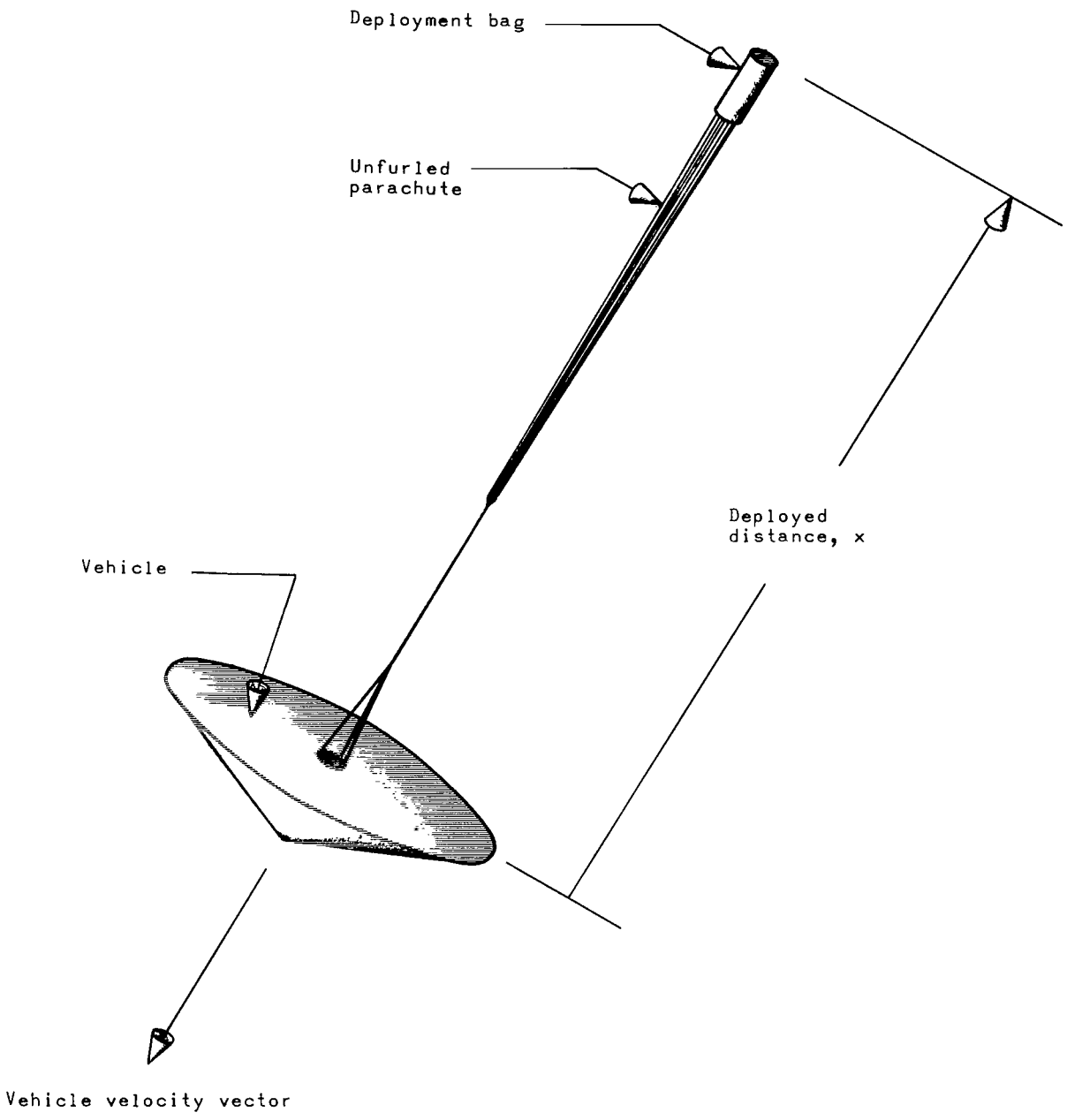

Figure 1.- Sketch of deployment configuration.

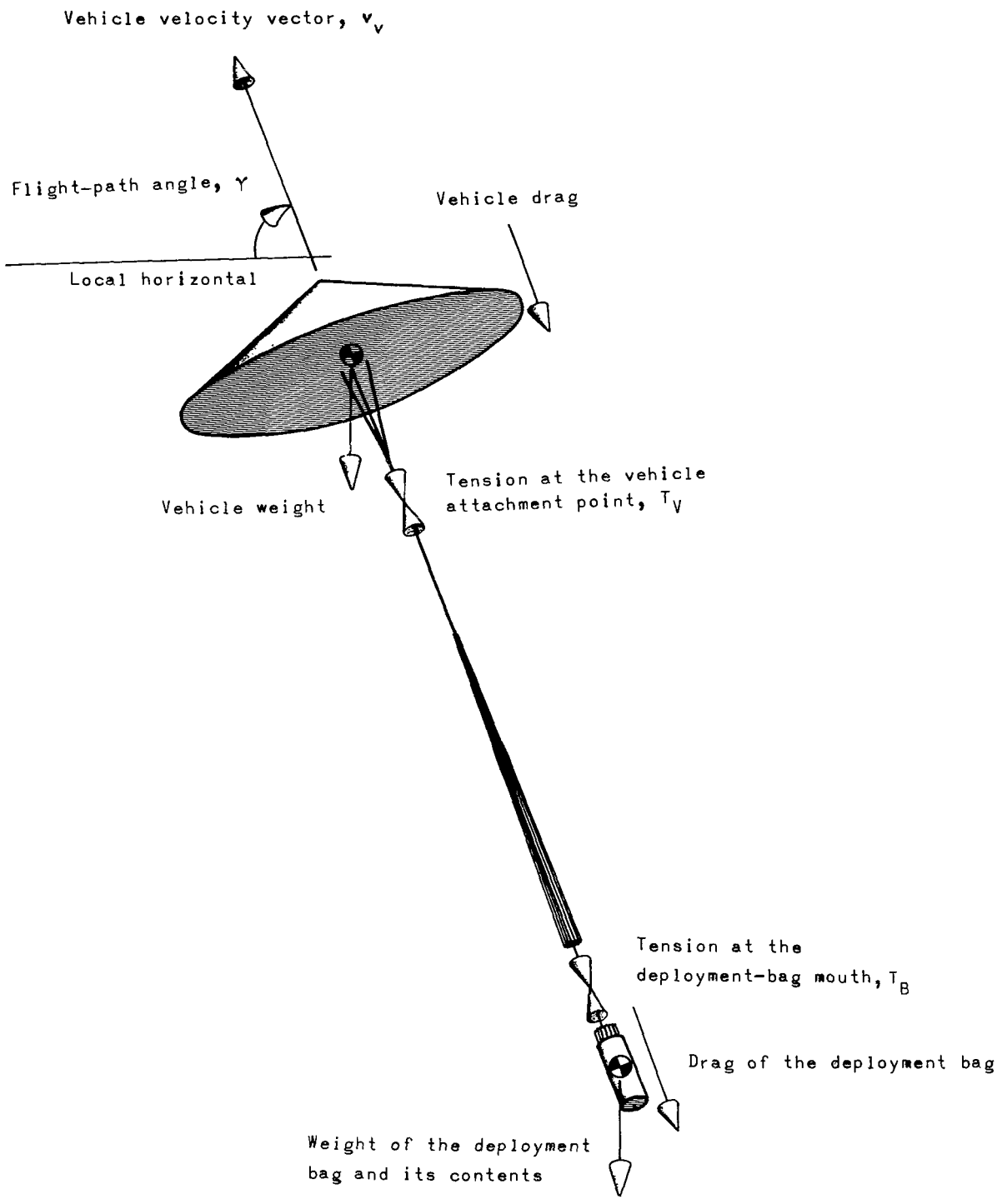

Figure 2.- Forces affecting the dynamics of parachute deployment.

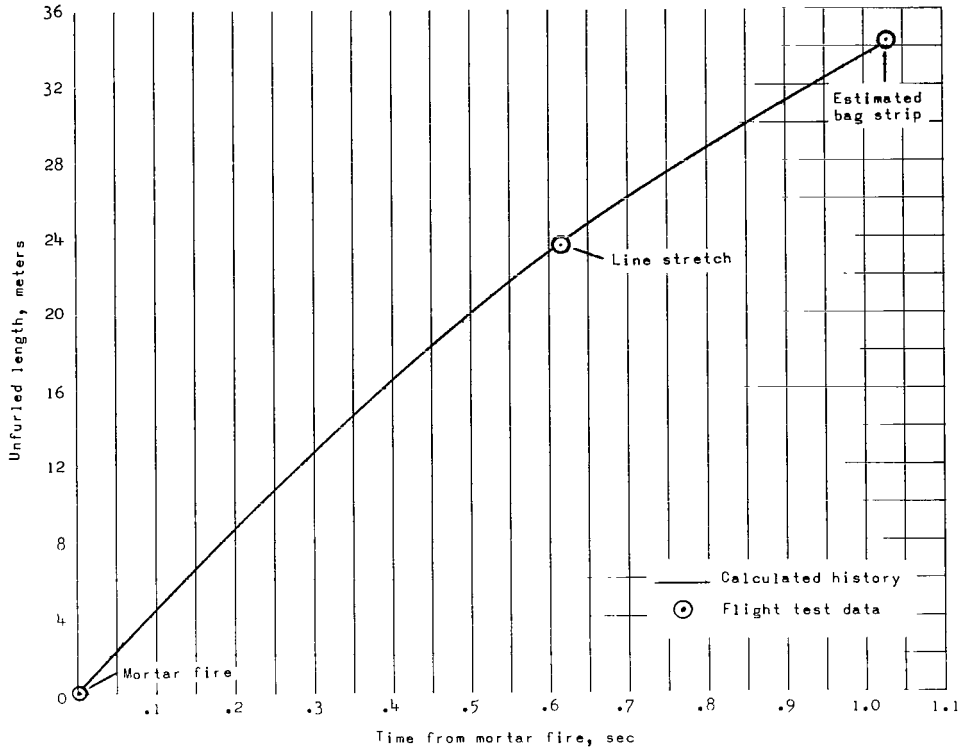

(a) Second balloon-launched flight test of Planetary Entry Parachute Program (ref. 6).

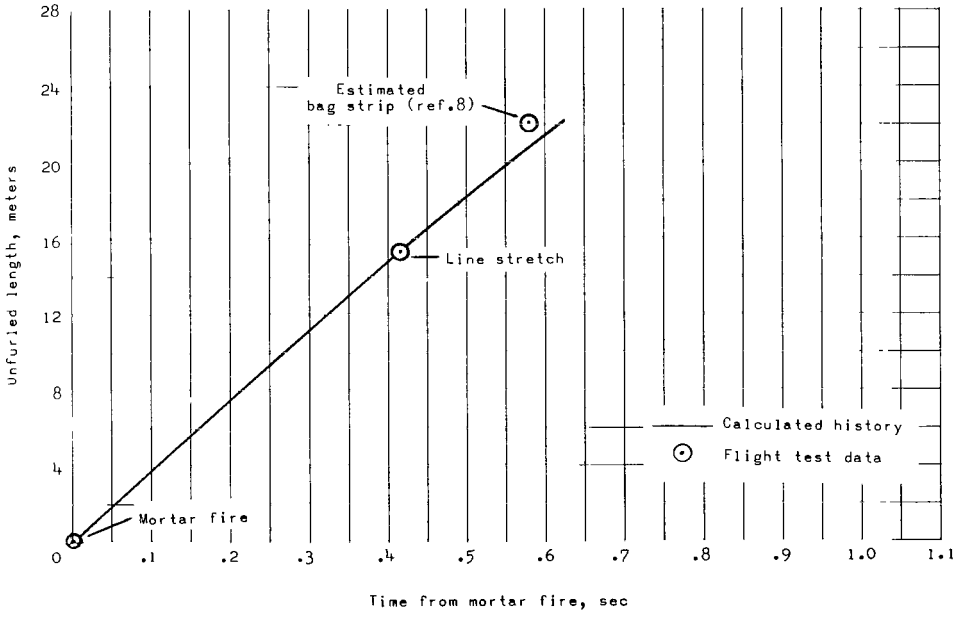

(b) First flight test of Supersonic Planetary Entry Decelerator Program (ref. 7).

Figure 3.- Comparison of calculated histories of unfurled length and flight test data for deployments of two disk-gap-band parachutes.

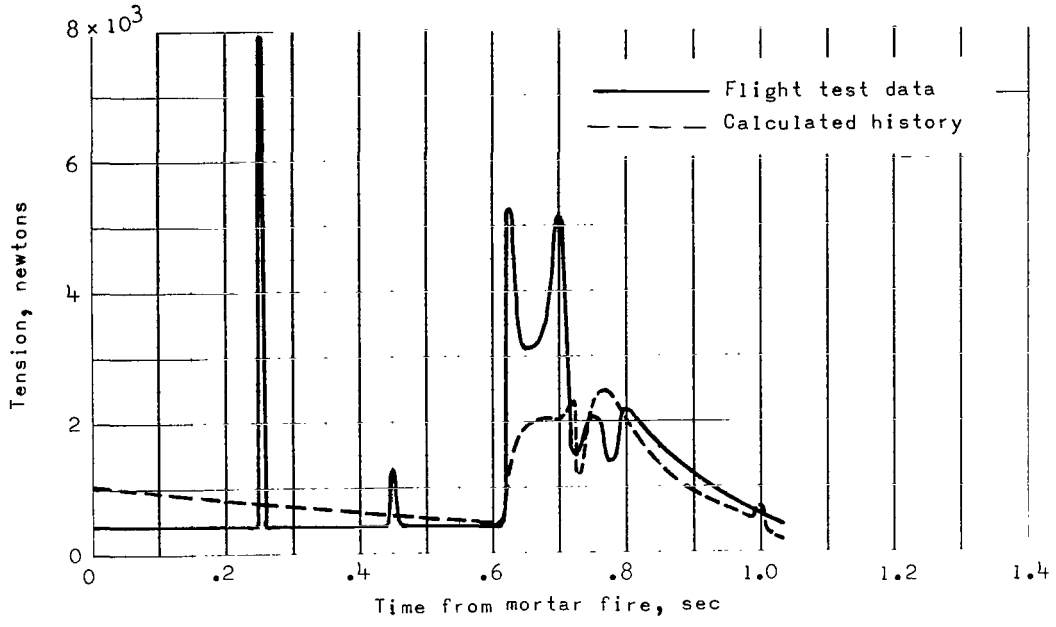

(a) Second balloon launched flight test of Planetary Entry Parachute Program (ref. 6).

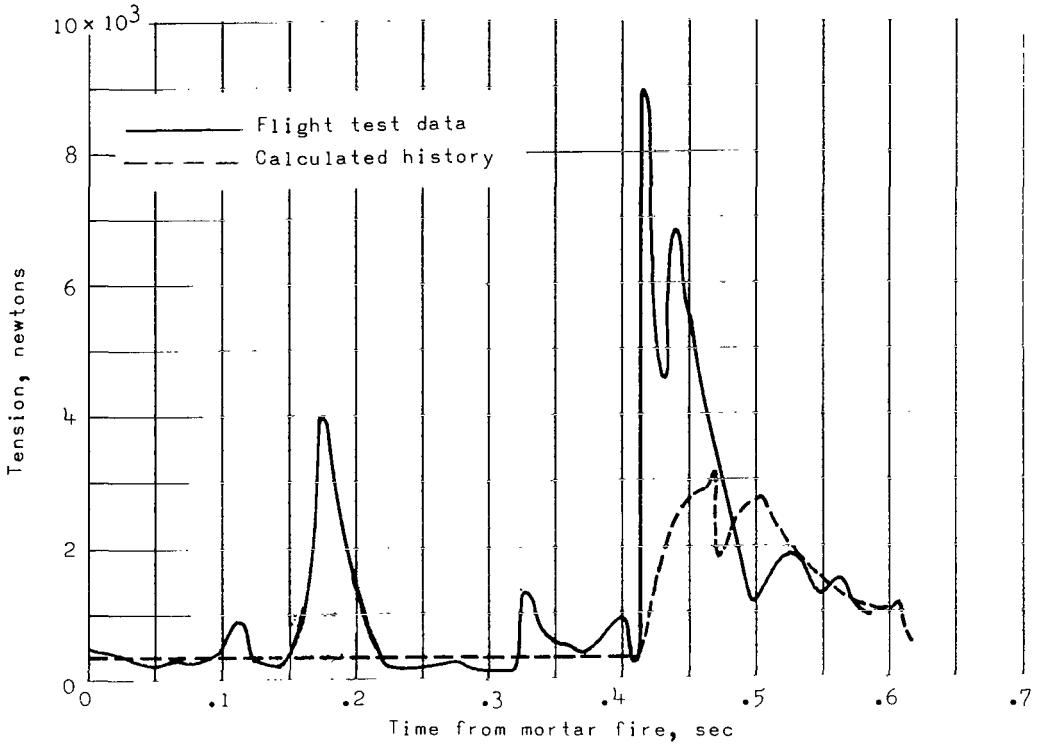

(b) First flight test of Supersonic Planetary Entry Decelerator Program (ref. 7).

Figure 4.- Comparison of calculated tension histories and flight test data for deployments of disk-gap-band parachutes.

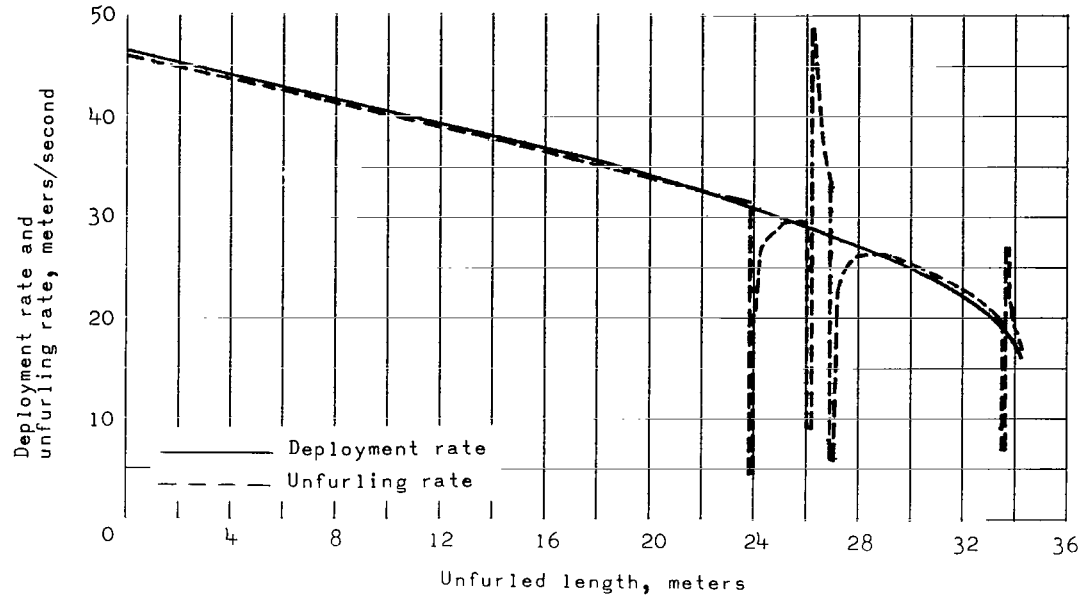

(a) Precise linear mass distribution.

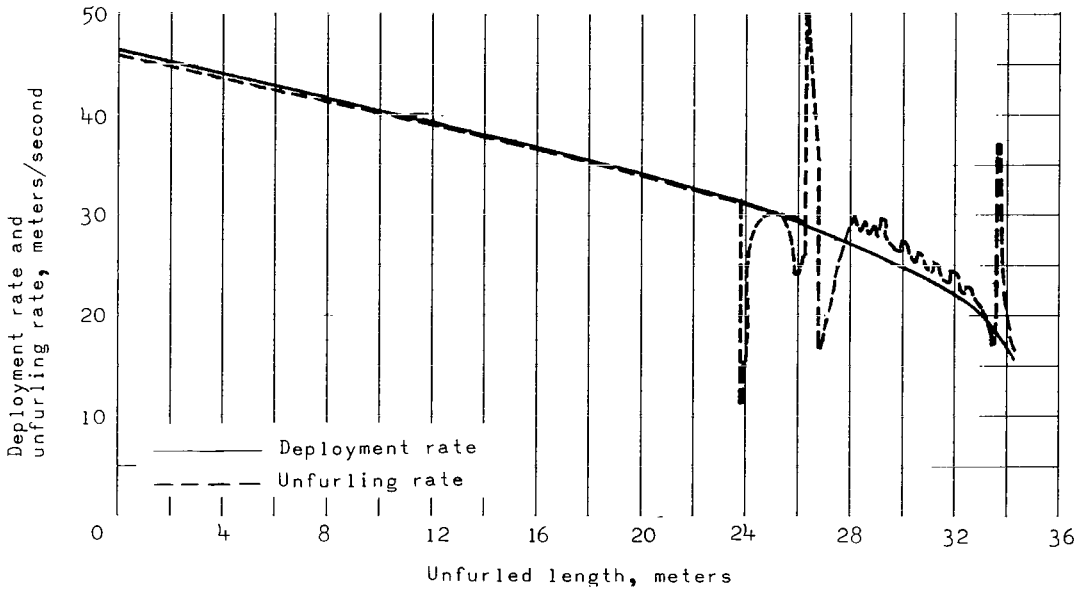

(b) Averaged linear mass distribution.

Figure 5.- Comparison of calculated deployment rate and unfurling rate, as influenced by different linear mass distributions, for the second balloon-launched flight test of the Planetary Entry Parachute Program (ref. 6).

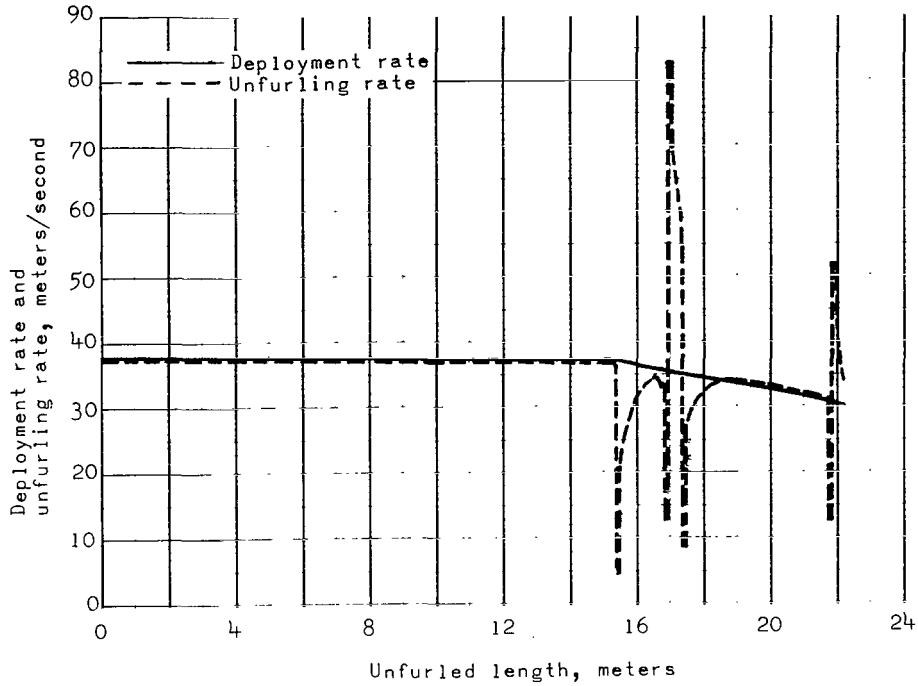

(a) Precise linear mass distribution.

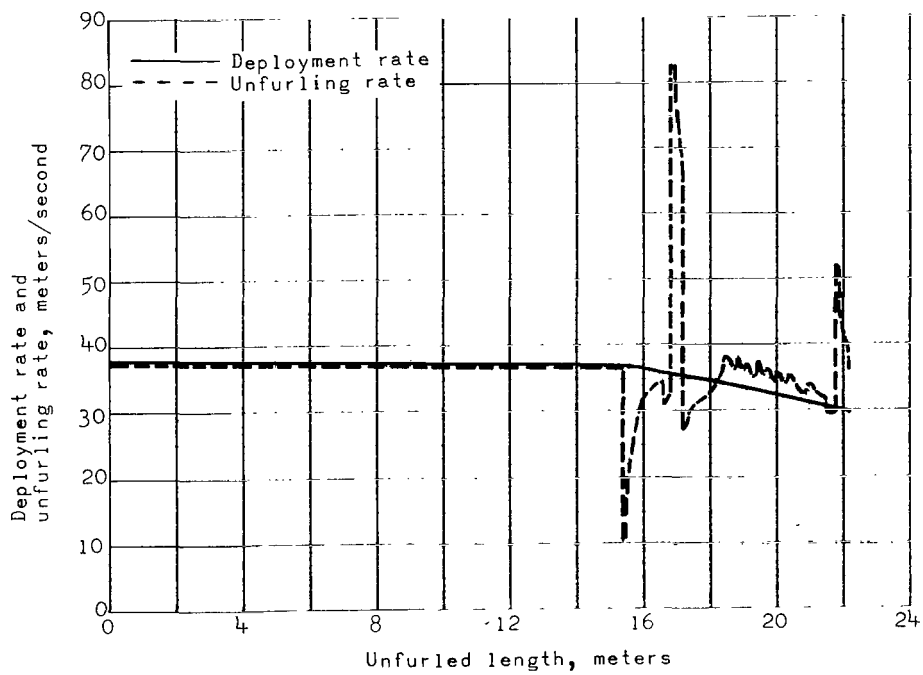

(b) Averaged linear mass distribution.

Figure 6.- Comparison of calculated deployment rate and unfurling rate, as influenced by different linear mass distributions, for the first flight test of the Supersonic Planetary Entry Decelerator Program (ref. 7).

NASA-Langley, 1972 —— 32 L-8097

"The aeronautical and space activities of the United States shall be conducted so as to contribute . . . to the expansion of human knowledge of phenomena in the atmosphere and space. The Administration shall provide for the widest practicable and appropriate dissemination of information concerning its activities and the results thereof."

—NATIONAL AERONAUTICS AND SPACE ACT OF 1958

NASA SCIENTIFIC AND TECHNICAL PUBLICATIONS

TECHNICAL REPORTS: Scientific and technical information considered important, complete, and a lasting contribution to existing knowledge.

TECHNICAL NOTES: Information less broad in scope but nevertheless of importance as a contribution to existing knowledge.

TECHNICAL MEMORANDUMS: Information receiving limited distribution because of preliminary data, security classification, or other reasons.

CONTRACTOR REPORTS: Scientific and technical information generated under a NASA contract or grant and considered an important contribution to existing knowledge.

TECHNICAL TRANSLATIONS: Information published in a foreign language considered to merit NASA distribution in English.

SPECIAL PUBLICATIONS: Information derived from or of value to NASA activities. Publications include conference proceedings, monographs, data compilations, handbooks, sourcebooks, and special bibliographies.

TECHNOLOGY UTILIZATION PUBLICATIONS: Information on technology used by NASA that may be of particular interest in commercial and other non-aerospace applications. Publications include Tech Briefs, Technology Utilization Reports and Technology Surveys.

Details on the availability of these publications may be obtained from:

SCIENTIFIC AND TECHNICAL INFORMATION OFFICE

NATIONAL AERONAUTICS AND SPACE ADMINISTRATION

Washington, D.C. 20546